PROCEEDINGS OF SCIENCE

# Recent quarkonium results from Belle II

**R. Garg on behalf of the Belle II collaboration**[a,*]

[a] *Carnegie Mellon University,*
*5000 Forbes Avenue, Pittsburgh, USA*

*E-mail:* renu2@andrew.cmu.edu

The Belle II experiment at the SuperKEKB energy-asymmetric $e^+e^-$ collider is the upgraded successor of the $B$-factory facility at the KEK laboratory, Japan. The first data taking period beyond the $\Upsilon(4S)$ peak energy has been devoted to the study of the region around $\sqrt{s}$ = 10.75 GeV, where enhanced transition rates to lower bottomonia suggested the existence of a new exotic bound state. This proceedings summarizes the most recent measurements of exotic quarkonium states to probe the fundamentals of QCD at the Belle II experiment.

*XVI International Conference on Heavy Quarks and Leptons (HQL 2023)*
*November 28, 2023 to December 2, 2023*
*TIFR, Mumbai, India*

*Supported by U. S. Dept. of Energy under contract number DE-SC-0010118

## 1. Introduction

Heavy quarkonium spectroscopy offers multiple opportunities to investigate the non-perturbative behavior of quantum chromodynamics. In recent years various collaborations, in particular those working at $e^+e^-$ colliders, discovered a number of unexpected quarkonium-like states, labeled as $X$, $Y$, and $Z$ states, in both the charmonium and bottomonium mass regions. Since these exotic hadrons are not predicted by the quark model, different compositions are being considered, such as compact tetraquarks, mesonic molecules and hybrids. More experimental results are needed in this sector for a better understanding of the phenomenology of quarkonium(-like) states and their transitions.

## 2. $\Upsilon(10753)$ state

The $\Upsilon(10753)$ bottomonium-like vector state was observed in the cross-section for the process of $e^+e^- \to \pi^+\pi^-\Upsilon(nS)$ ($n$ = 1, 2, 3) by Belle [1] and in fits to the $e^+e^- \to b\bar{b}$ cross-sections at energies $\sqrt{s}$ from 10.52 to 11.02 GeV [2]. The mass and width of this state are $M = (10753 \pm 6)$ MeV/c$^2$ and $\Gamma = (36^{+18}_{-12})$ MeV, respectively. This mass is not consistent with any of the predicted states, which makes it difficult to assign the $\Upsilon(10753)$ as a conventional bottomoium state. The unknown nature of the $\Upsilon(10753)$ state is generating a wide interest on the theoretical side. As the newly observed state does not correspond to any pure $b\bar{b}$ resonance, the most popular interpretations describe the $\Upsilon(10753)$ as a mixture of $\Upsilon(4S)$ and $\Upsilon(3D)$ states [3, 4]. Several other interpretations consider the state as a conventional bottomonium [5–10], hybrid [11], hadronic molecule with a small admixture of a bottomonium [12], or tetraquark state [13, 14], but there is no definitive explanation so far.

Further measurements of the properties and decay modes of the $\Upsilon(10753)$ are important to advance our understanding of its nature and test theoretical predictions. Therefore, to confirm the existence of this new state and study its properties, Belle II performed an energy scan in the proximity of the $\Upsilon(10753)$, collecting 19.3 fb$^{-1}$ at the four center-of-mass (c.m.) energy points $\sqrt{s}$ = 10.653, 10.701, 10.745, 10.805 GeV.

### 2.1 Study of $\Upsilon(10753) \to (\pi^+\pi^-\pi^0)\gamma\Upsilon(1S)$

One interpretation of the $\Upsilon(10753)$ as an admixture of $\Upsilon(4S)$ and $\Upsilon(3D)$ states predicts comparable branching fractions of $10^{-3}$ for $\Upsilon(10753) \to \omega\chi_{bJ}$ and $\Upsilon(10753) \to \pi^+\pi^-\Upsilon(nS)$. Also, the branching fraction for $\Upsilon(10753) \to \omega\chi_{b1}$ is expected to be about 1/5 of that for $\Upsilon(10753) \to \omega\chi_{b2}$ [7]. In addition, the process $\Upsilon(10753) \to \gamma X_b$, $X_b \to \omega\Upsilon(1S)$, which shares the same final states as $\Upsilon(10753) \to \omega\chi_{bJ}$, provides access to the $X_b$. The $X_b$ is the bottomonium analogue of the $X(3872)$. Its existence has been predicted in molecular [15–17] and tetraquark models [18–20].

The reaction $e^+e^- \to \gamma\omega\Upsilon(1S)$ is quite promising because it can result from two of the above-mentioned decay modes: the $\omega\chi_{bJ}$ transition and the search for the bottomonium analogue of the $X(3872)$, which is expected to decay to $X_b \to \omega\Upsilon(1S)$.

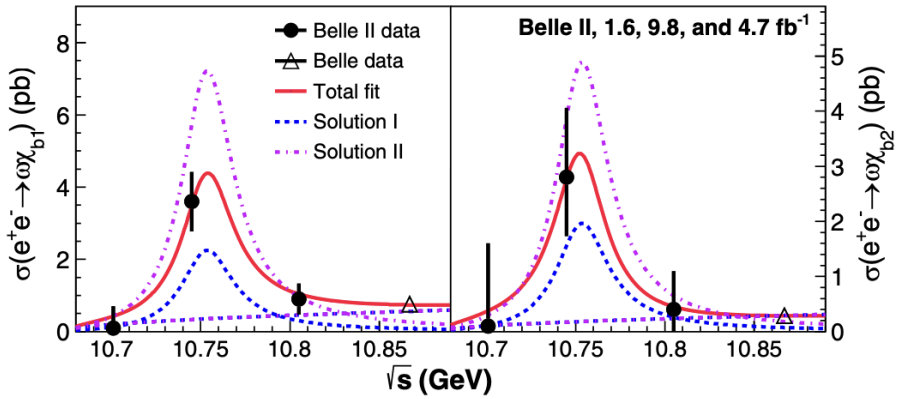


**Figure 1:** Energy dependence of the Born cross sections for $e^+e^- \to \omega\chi_{b1}$ (left) and $e^+e^- \to \omega\chi_{b2}$ (right). Circles show our measurements and triangles are the results of the Belle experiment [22]. Error bars represent combined statistical and systematic uncertainties. Curves show the fit results and various components of the fit function, where the two solutions correspond to the two signs of interference.

A significant $\omega\chi_{b1}$ signal and evidence for the $e^+e^- \to \omega\chi_{b2}$ process at $\sqrt{s} = 10.745$ GeV are found. The corresponding Born cross sections ($\sigma$) are calculated using

$$\sigma = \frac{N}{L\epsilon}$$

where, $N$ is the yield of a specific decay mode, $L$ is the integrated luminosity and $\epsilon$ is the reconstruction efficiency. The Born cross sections for $e^+e^- \to \omega\chi_{b1}$ and $e^+e^- \to \omega\chi_{b2}$ are $(3.6 \pm 0.7 \pm 0.5)$ pb and $(2.8^{+1.2}_{-1.0} \pm 0.4)$ pb, respectively and shown in Fig. 1 as function of collision energy. We observe a strong enhancement of the cross section near 10.75 GeV.

We also measured the ratio $\sigma_B(e^+e^- \to \omega\chi_{b1})/\sigma_B(e^+e^- \to \omega\chi_{b2}) = 1.3 \pm 0.6$ at $\sqrt{s} = 10.745$ GeV, where the statistical uncertainties and systematic uncertainties are included. This observed ratio contradicts the expectation for a pure $D$-wave bottomonium state of 15 [21] and there is also a $1.8\sigma$ difference with the prediction of 0.2 for a $S - D$ mixed state [7].

The distributions of $M[\omega\Upsilon(1S)]$ for events within $0.70 < M(\pi^+\pi^-\pi^0) < 0.86$ GeV/$c^2$ at $\sqrt{s} =$ 10.653, 10.701, 10.745, and 10.805 GeV are shown in Fig. 2. The reflections of the $e^+e^- \to \omega\chi_{bJ}$ signals are observed, but no evidence of a $X_b$ signal is obtained for $X_b$ masses between 10.45 and 10.65 GeV/$c^2$. The upper limits at 90% Bayesian confidence on the products of Born cross section for $e^+e^- \to \gamma X_b$ and branching fraction for $X_b \to \omega\Upsilon(1S)$ are set to be 0.55, 0.84, 0.14, and 0.37 pb at 10.653, 10.701, 10.745, and 10.805 GeV, respectively.

### 2.2 Study of $\Upsilon(10753) \to \omega\chi_{b0}(1P)/\omega\eta_b(1S)$

We next report on a search for the processes $e^+e^- \to \omega\eta_b(1S)$ and $e^+e^- \to \omega\chi_{b0}(1P)$ at a c.m. energy of 10.745 GeV, which is close to the peak of the $\Upsilon(10753)$ state. The $\eta_b(1S)$ and $\chi_{b0}(1P)$ mesons do not have exclusive decay channels with a large product of efficiency and branching fraction. Thus, we reconstruct only an $\omega$ meson in the $\pi^+\pi^-\pi^0$ decay and use recoil

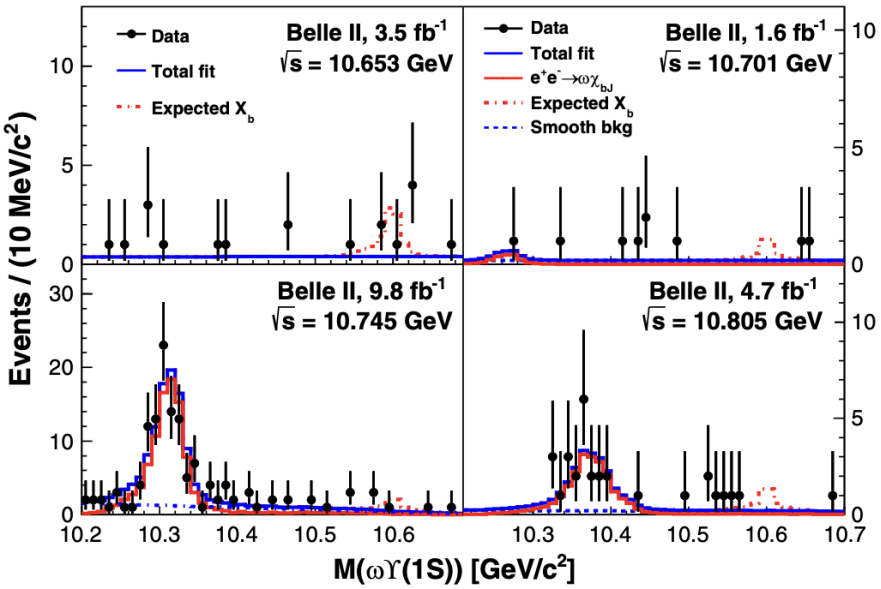


**Figure 2:** Distributions of $\omega\Upsilon(1S)$ mass from data at $\sqrt{s}$ = 10.653, 10.701, 10.745, and 10.805 GeV. The red dash-dotted histograms are from simulated events $\Upsilon(10753) \to \gamma X_b$, $X_b \to \omega\Upsilon(1S)$ with the $X_b$ mass fixed at 10.6 GeV/$c^2$ and yields fixed at the upper limit values. The red soild line is the reflection of the $e^+e^- \to \omega\chi_{bJ}$ signals.

mass,

$$M_{\rm recoil}(\pi^+\pi^-\pi^0) = \sqrt{\left(\frac{\sqrt{s}-E_\omega}{c^2}\right)^2 - \left(\frac{p_\omega}{c}\right)^2} \qquad (1)$$

as the signal extraction variable, where $E_\omega$ and $p_\omega$ are the energy and momentum of the $\pi^+\pi^-\pi^0$ combination in the c.m. frame. In a previous study [23], we searched for the process $e^+e^- \to \omega\chi_{b0}(1P)$ fully reconstructing the $\chi_{b0}(1P) \to \gamma\Upsilon(1S)$ decay and found no significant signal. The probability of the decay $\chi_{b0}(1P) \to \gamma\Upsilon(1S)$ is small, thus, the sensitivity of partial reconstruction, applied in this analysis, might be higher than that of full reconstruction.

The fit results of the $M_{\rm recoil}(\pi^+\pi^-\pi^0)$ for the $e^+e^- \to \omega\eta_b(1S)$ and $e^+e^- \to \omega\chi_{b0}(1P)$ decays are shown in Fig. 3. No significant signals are observed. Therefore, we set the 90% confidence level upper limits on the Born-level cross sections:

$$\sigma_B(e^+e^- \to \omega\eta_b(1S)) < 2.5 \text{ pb},$$

$$\sigma_B(e^+e^- \to \omega\chi_{b0}(1P)) < 8.7 \text{ pb}.$$

The upper limit on the $e^+e^- \to \omega\chi_{b0}(1P)$ cross section is comparable to the upper limit obtained using full reconstruction of 11.3 pb [23]. The tetraquark model [13] predicts that the decay rate of $\Upsilon(10753) \to \omega\eta_b(1S)$ should be strongly enhanced compared to the decay rates of $\Upsilon(10753) \to \pi^+\pi^-\Upsilon(nS)$. The obtained upper limit on $\sigma_B(\omega\eta_b(1S))$ is close to the measured values of $\sigma_B(\pi^+\pi^-\Upsilon(nS))$, which are in the range (1 − 3) pb [1]. Thus, our results do not support the tetraquark-model prediction that the $\Upsilon(10753) \to \omega\eta_b(1S)$ decay is enhanced [13]. In the

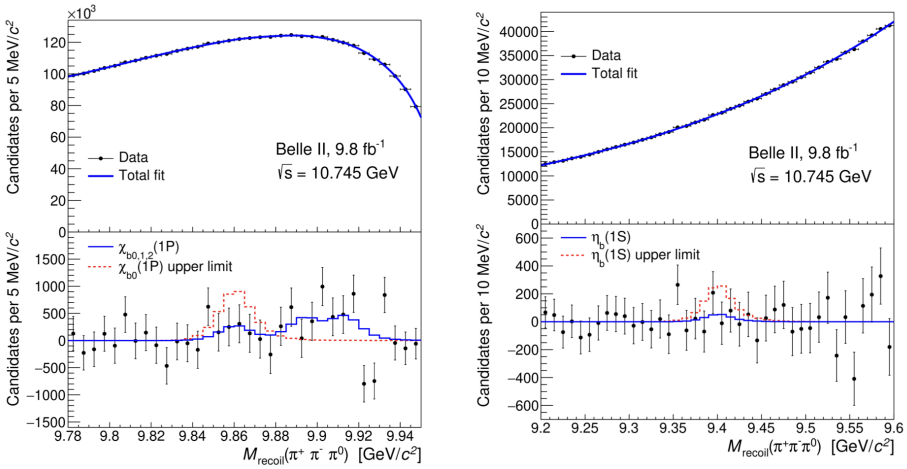


**Figure 3:** Distribution of $M_{\text{recoil}}(\pi^+\pi^-\pi^0)$ for the $e^+e^- \to \omega\eta_b(1S)$ (left) and $e^+e^- \to \omega\chi_{b0}(1P)$ (right) candidates. Top distributions are data points with the fit function overlaid and the bottom are the same distributions with the background component of the fit function subtracted. The solid histogram shows the fit function for the best fit; the dashed histogram shows the same function with the yield fixed to the upper limit.

$4S-3D$ mixing model, the decay rate of $\Upsilon(10753) \to \omega\eta_b(1S)$ is smaller than the decay rate of $\Upsilon(10753) \to \pi^+\pi^-\Upsilon(nS)$ by a factor $0.2-0.4$ [24]; our upper limit does not contradict this expectation.

The upper limit on the $\omega\chi_{b0}(1P)$ cross section is higher than the measured $\omega\chi_{b1}(1P)$ and $\omega\chi_{b0}(1P)$ cross sections of $(3.6\pm0.9)$ pb and $(2.8\pm1.3)$ pb, respectively [23]. For a $4S-3D$ mixed state, the decay rate to $\omega\chi_{b0}(1P)$ is expected to be comparable to the decay rates to $\omega\chi_{b1}(1P)$ and $\omega\chi_{b2}(1P)$ [8]; our upper limit is consistent with this expectation. In the charmonium sector, the decay of the $Y(4230)$ state to $\omega\chi_{c0}$ is enhanced compared to the decays to $\omega\chi_{c1}$ and $\omega\chi_{c2}$ [25]. We do not find an analogous enhancement in the decay pattern of $\Upsilon(10753)$, which may indicate that the $Y(4230)$ and $\Upsilon(10753)$ have different structures.

### 2.3 Study of $\Upsilon(10753) \to \pi^+\pi^-\Upsilon(nS)$

We present an analysis of $\Upsilon(10753) \to \pi^+\pi^-\Upsilon(nS)$ using new, large samples of data collected explicitly for this purpose by the Belle II experiment. We reconstruct decays to the $\pi^+\pi^-\Upsilon(nS)$ final state, with $\Upsilon(nS)$ decaying to a $\mu^+\mu^-$ pair, at $\sqrt{s}$ from $10.6-10.8$ GeV. We calculate and fit the Born cross sections, $\sigma_B$, for these processes as a function of $\sqrt{s}$ to measure the $\Upsilon(10753)$ mass and width. We also search for intermediate states to study the internal decay dynamics (e.g., $e^+e^- \to f_0(980)[\to \pi^+\pi^-]\Upsilon(nS)$) and exotic states ($e^+e^- \to \pi^\mp Z_b(10610, 10650)^\pm[\to \pi^\pm\Upsilon(nS)]$), which may provide deeper understanding into the possibility of an unconventional nature for the $\Upsilon(10753)$.

The Born cross sections and the fit to their energy dependence are displayed in Fig. 4. Signals for the $\Upsilon(10753)$ are observed in $\pi^+\pi^-\Upsilon(1S)$ and $\pi^+\pi^-\Upsilon(2S)$ with greater than $8\sigma$ significance, while no evidence is found for $\pi^+\pi^-\Upsilon(3S)$.

The cross-section ratios $\sigma(\pi^+\pi^-\Upsilon(1S,3S))/\sigma(\pi^+\pi^-\Upsilon(2S))$ at the $\Upsilon(10753)$ resonance peak are determined for the first time. The values are $0.46^{+0.15}_{-0.12}$ and $0.10^{+0.05}_{-0.04}$ for $\pi^+\pi^-\Upsilon(1S)$ and

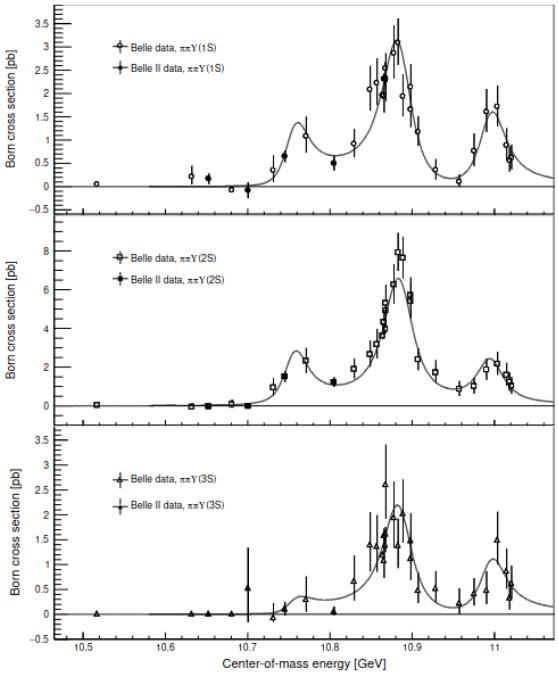


**Figure 4:** Born cross sections for $\pi^+\pi^-\Upsilon(1S)$ (top), $\pi^+\pi^-\Upsilon(2S)$ (middle), and $\pi^+\pi^-\Upsilon(3S)$ (bottom), with fit results overlaid.

$\pi^+\pi^-\Upsilon(3S)$, respectively. The ratio for $\pi^+\pi^-\Upsilon(1S)$ is compatible with the ratios at the $\Upsilon(5S)$ and $\Upsilon(6S)$ resonance peaks. However, the relative ratio of $\pi^+\pi^-\Upsilon(3S)$ at the $\Upsilon(10753)$ peak is about $3-4$ times smaller than those at the $\Upsilon(5S)$ and $\Upsilon(6S)$ peaks.

The distributions of $M(\pi^+\pi^-)$ (left) and $\Delta M_\pi$ (right) for events in the signal regions are shown in Fig. 5, compared with the events from sideband regions. We did not find any evidence that these transitions occur via intermediate $Z_b(10610, 10650)^\pm$ states. The dipion invariant mass in $\pi^+\pi^-\Upsilon(1S)$ (Fig. 5, top-left) is consistent with the simulated phase-space distribution. The dipion invariant mass in $\pi^+\pi^-\Upsilon(2S)$ (Fig. 5, bottom-left) production is similar to that observed in the $\Upsilon(2S) \to \pi^+\pi^-\Upsilon(1S)$ process and can be described accurately by the $\Upsilon(nS)$ transition amplitude. This distribution can provide an input for theoretical calculations.

The mass and width of $\Upsilon(10753)$ are measured to be $(10756.3 \pm 2.7 \pm 0.6)$ MeV/c$^2$ and $(29.7 \pm 8.5 \pm 1.1)$ MeV, respectively, which are consistent with previous measurements but with uncertainties nearly a factor of two smaller. These results supersede the previous Belle result [1]. This improvement in accuracy provides a more precise comparison for theoretical calculations.

## 3. Energy dependence of $e^+e^- \to B^{(*)}\bar{B}^{(*)}$ cross-section

These open-flavor final states, $B^{(*)}\bar{B}^{(*)}$, are expected to be the dominant decay channels for $b\bar{b}$ hadrons and constitute the main contribution to the total $b\bar{b}$ cross section. Thus, measuring the exclusive $e^+e^- \to B^{(*)}\bar{B}^{(*)}$ cross sections provides important information on the interactions in this energy region and in particular about the structure of bottomonium(-like) resonances. The measured cross sections can be used in the coupled channel analysis of all available scan data to

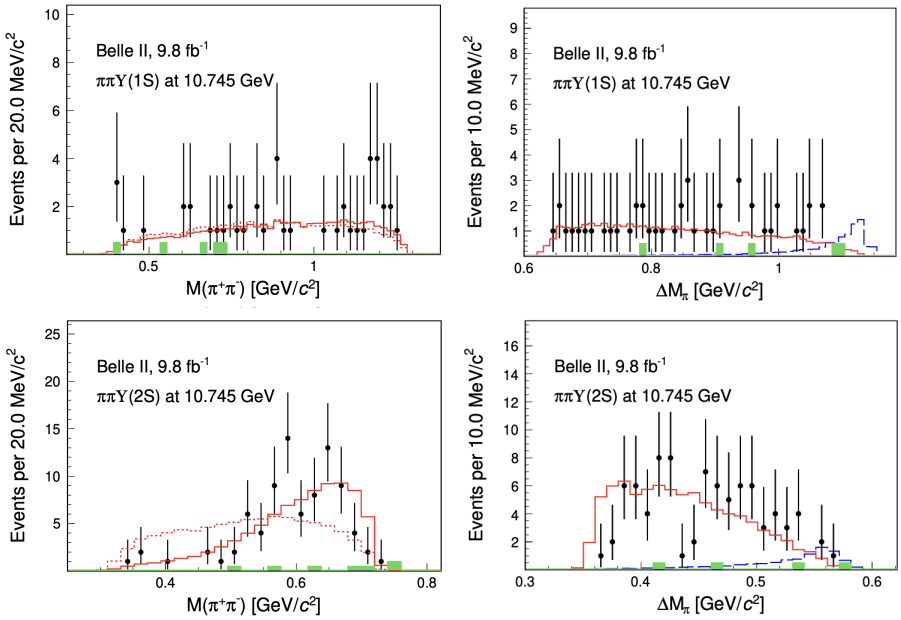


**Figure 5:** Distributions of dipion mass (left) and maximal difference between the $\pi^+\pi^-\mu^+\mu^-$ mass and the $\pi^\pm\mu^+\mu^-$ mass (right). Plots from top to bottom show $\pi^+\pi^-\Upsilon(1S)$ and $\pi^+\pi^-\Upsilon(2S)$ at $\sqrt{s}$ = 10.745 GeV, respectively. Points with error bars show the events in the signal region from data, green shaded histograms show the events in the sideband region, red histograms the weighted simulated signal, red dotted histogram is the phase space signal MC simulation, and blue dashed histogram is the $Z_b(10610/10650)^\pm$ from MC simulation.

extract the parameters of the $b\bar{b}$ states. This topic is of special interest since all the states above threshold exhibit anomalies, especially in transitions to lower bottomonia, which currently are not well understood. The analysis follows the analogous measurement performed at Belle [26], where the measured energy dependencies of $\sigma(e^+e^- \to B^{(*)}\bar{B}^{(*)})$ showed an oscillatory behavior.

In this paper, we report the measurement of the energy dependence of the $e^+e^- \to B\bar{B}$, $e^+e^- \to B\bar{B}^*$, and $e^+e^- \to B^*\bar{B}^*$ exclusive cross sections. Our approach is to perform a full reconstruction of one $B$ meson in hadronic channels, and then to identify the $B\bar{B}$, $B\bar{B}^*$, and $B^*\bar{B}^*$ signals using the $M_{\rm bc}$ distribution, $M_{\rm bc} = \sqrt{(E_{cm}/2)^2 - p_B^2}$, where $E_{cm}$ is the c.m. energy and $p_B$ is the $B$-candidate momentum measured in the c.m. frame. The $M_{\rm bc}$ distribution for $B\bar{B}$ events peaks at the nominal $B$-meson mass, $m_B$, while the distributions for $B\bar{B}^*$, and $B^*\bar{B}^*$ events peak approximately at $m_B - \Delta m_{B^*}/2$ and $m_B - \Delta m_{B^*}$, respectively, where $\Delta m_{B^*}$ is the mass difference of the $B^*$ and $B$ mesons. The $M_{\rm bc}$ distribution obtained at $\sqrt{s}$ = 10.746 GeV is shown in Fig. 6 left.

The signal yields are estimated by fitting the $M_{\rm bc}$ distributions. The fit function for the signal and peaking background components is constructed in the same way as in Ref. [26]. From the yield $N$ of a specific decay mode, the corresponding dressed cross section is calculated as

$$\sigma^{\rm dressed} = \frac{N}{(1+\delta_{ISR})L\epsilon}$$

where $(1+\delta_{ISR})$ is the radiative correction factor, $L$ is the integrated luminosity and $\epsilon$ is the reconstruction efficiency. We fit simultaneously the energy dependence of the $e^+e^- \to B\bar{B}$,

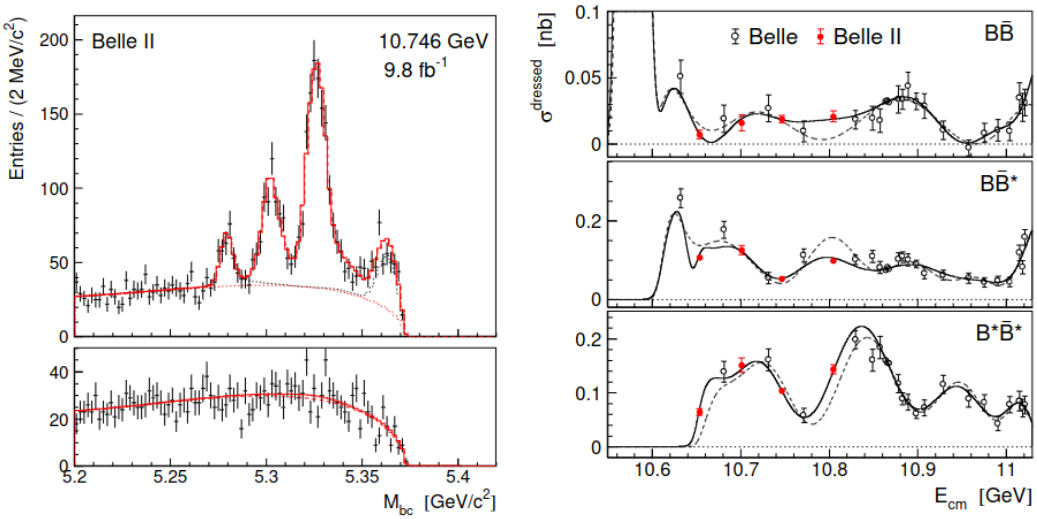


**Figure 6:** Results of the measurement of the $e^+e^- \to B\bar{B}$, $e^+e^- \to B\bar{B}^*$, and $e^+e^- \to B^*\bar{B}^*$ cross sections using the Belle II scan data. The signal yields are obtained by fitting the $M_{\rm bc}$ distributions (left) at each value of $\sqrt{s}$ and the energy dependence of the Born cross section (right), combined with the measurement from Belle.

$e^+e^- \to B\bar{B}^*$, and $e^+e^- \to B^*\bar{B}^*$ cross sections and of the total $e^+e^- \to b\bar{b}$ cross section. The results are shown in Fig. 6 right, where the previous measurements from Belle are included.

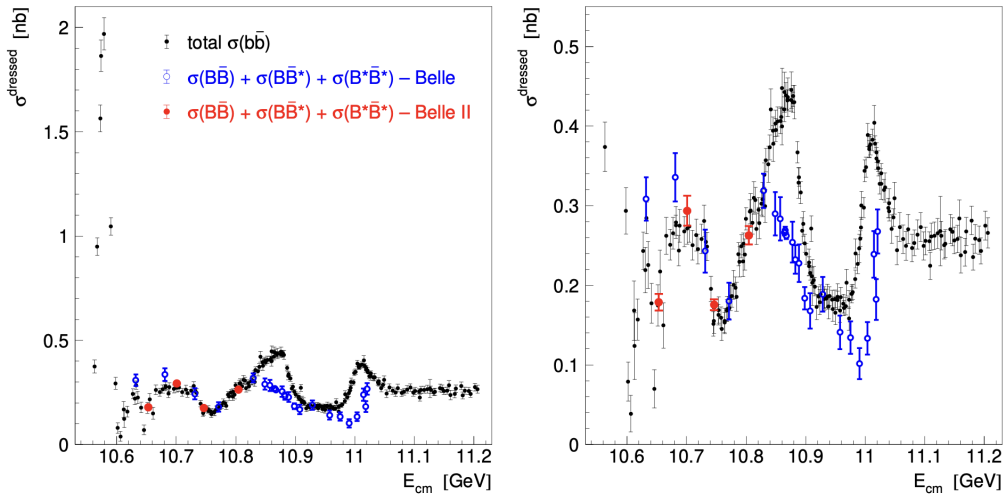


**Figure 7:** Energy dependence of the total $b\bar{b}$ dressed cross section obtained in Ref. [2] from the visible cross sections measured by Belle [28], and BaBar [27] (black circles) and the sum of the exclusive $B\bar{B}$, $B\bar{B}^*$, and $B^*\bar{B}^*$ cross sections measured by Belle [26] (open blue circles) and in this work (filled red circles). The right panel shows the low cross-section region with an expanded scale.

In Fig. 7 we show the sum of the exclusive $B\bar{B}$, $B\bar{B}^*$, and $B^*\bar{B}^*$ cross sections measured in this work and in the Belle experiment [26], superimposed on the total $b\bar{b}$ dressed cross section [2]. The sum of measurements performed in this work agrees well with the total cross section. The

deviation at higher energy is presumably due to the contribution of $B_s^0$ mesons, multibody final states $B^{(*)}\bar{B}^{(*)}\pi(\pi)$, and production of bottomonia in association with light hadrons.

## 4. Summary

We have shown recent measurements performed by the Belle II collaboration using the data set collected in an energy scan above the $\Upsilon(4S)$ resonance. These results are of great importance in understanding the nature of the new $\Upsilon(10753)$ state and, more generally, of the bottomonium(-like) states above the open flavor threshold. The present status of the $\Upsilon(10753)$ is shown in Fig. 8. The uniqueness of the data set collected at center-of-mass energies around 10.75 GeV will enable Belle II to provide further unprecedented results in the quarkonium sector in the near future.

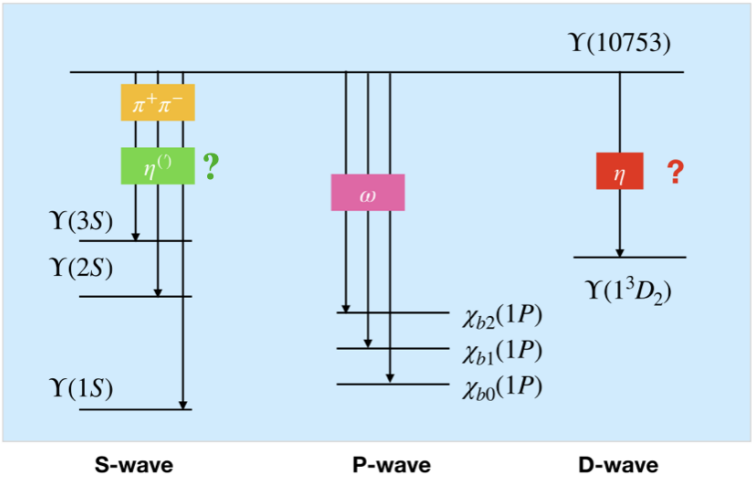


**Figure 8:** Present status of $\Upsilon(10753)$ state.

## References

[1] R. Mizuk *et al.* (Belle Collaboration), J. High Energy Phys. **10** (2019) 220.

[2] X. K. Dong, X. H. Mo, P. Wang, and C. Z. Yuan, Chin. Phys. C **44** (2020) 083001.

[3] J. F. Giron and R. F. Lebed, Phys. Rev. D **102** (2020) 014036.

[4] B. Chen, A. L. Zhang, and J. He, Phys. Rev. D **101** (2020) 014020.

[5] Q. Li, M. S. Liu, Q. F. Lü, L. C. Gui, and X. H. Zhong, Eur. Phys. J. C **80** (2020) 59.

[6] W. H. Liang, N. Ikeno, and E. Oset, Phys. Lett. B **803** (2020) 135340.

[7] Y. S. Li, Z. Y. Bai, Q. Huang, and X. Liu, Phys. Rev. D **104** (2021) 034036.

[8] Z. Y. Bai, Y. S. Li, Q. Huang, X. Liu, and T. Matsuki, Phys. Rev. D **105** (2022) 074007.

[9] N. Hüsken, R. E. Mitchell, and E. S. Swanson, Phys. Rev. D **106** (2022) 094013.

[10] V. Kher, R. Chaturvedi, N. Devlani, and A. K. Rai, Eur. Phys. J. Plus **137** (2022) 357.

[11] N. Brambilla, W. K. Lai, J. Segovia, J. T. Castellà, and A. Vairo, Phys. Rev. D **99** (2019) 014017.

[12] P. Bicudo, N. Cardoso, L. Müller, and M. Wagner, Phys. Rev. D **103** (2021) 074507.

[13] Z. G. Wang, Chin. Phys. C **43** (2019) 123102.

[14] A. Ali, L. Maiani, A. Y. Parkhomenko, and W. Wang, Phys. Lett. B **802** (2020) 135217.

[15] N. A. Tornqvist, Z. Phys. C **61** (1994) 525.

[16] F. K. Guo, C. H. Duque, J. Nieves, and M. P. Valderrama, Phys. Rev. D **88** (2013) 054007.

[17] M. Karliner and S. Nussinov, J. High Energy Phys. **07** (2013) 153.

[18] D. Ebert, R. N. Faustov, and V. O. Galkin, Phys. Lett. B **634** (2006) 214.

[19] D. Ebert, R. N. Faustov, and V. O. Galkin, Mod. Phys. Lett. **24A** (2009) 567.

[20] A. Ali, C. Hambrock, I. Ahmed, and M. J. Aslam, Phys. Lett. B **684** (2010) 28.

[21] F. K. Guo, Ulf-G. Meißner, and C. P. Shen, Phys. Lett. B **738** (2014) 172.

[22] X. H. He *et al.* (Belle Collaboration), Phys. Rev. Lett. **113** (2014) 142001.

[23] I. Adachi *et al.* (Belle II Collaboration), Phys. Rev. Lett. **130** (2023) 091902.

[24] S. Liu, Z. Cai, Z. Jia, G. Li and J. Xie, arXiv:2312.02761563.

[25] M. Ablikim *et al.* (BESIII Collaboration), Phys. Rev. D **99** (2019) 091103.

[26] R. Mizuk *et al.* (Belle Collaboration), J. High Energy Phys. **06** (2021) 137.

[27] B. Aubert *et al.* (BaBar Collaboration), Phys. Rev. Lett. **102** (2009) 012001.

[28] D. Santel *et al.* (Belle Collaboration), Phys. Rev. D **93** (2016) 011101.